appears to be quite slow. The only conclusion that can safely be drawn at this stage is that, while the chemical and redox reactivities of the nitro and nitrosyl metallopolymers are maintained in solution, the film environment must play a major role in either altering or eliminating the usual reactivity of the sites.

Conclusions

We have prepared a series of metallopolymers and investigated their chemical and physical properties. The work has led to a number of important conclusions which are summarized below:

(1) Preparation of the metallopolymers can be accomplished by using synthetic procedures that are based on the known chemistry of monomeric analogues.

(2) The polymer-bound metal complex sites retain the chemical and physical properties inherent in related monomers, as shown by spectral measurements and the observation of net reactions of the various materials in homogeneous solutions.

(3) Interestingly, modifications in the chemical and redox reactivities of the polymer-bound sites do occur in certain cases when the metallopolymers are examined as films evaporatively deposited onto electrode surfaces. The origin of the differences is believed to be due to two major factors:

(A) *Spatial separation* of the chemical sites along the polymer chain can change the net chemistry by slowing or eliminating bimolecular reactions with strict orientational demands, e.g.

$$Ru^{III}(bpy)_2(PVP)(ONO)^{2+} + Ru^{III}(bpy)_2(PVP)(NO_2)^{2+} \rightarrow Ru^{II}(bpy)_2(PVP)(ONO_2)^{+} + Ru^{II}(bpy)_2(PVP)(NO)^{3+}$$

(B) Changes in the *local environment* at the chemical sites due to the presence of protonated or unprotonated pyridyl groups from the main chain of the polymer can also change the net chemistry, e.g.: (i) the loss of pH dependence for the Ru(III/II) couple of $Ru(bpy)_2(PVP)(OH_2)^{2+}$ at pH >4; (ii) the change in the course of the decomposition chemistry of $Ru(bpy)_2(PVP)(N_3)^{2+}$, where a labile intermediate appears to be captured by an unbound pyridyl group rather than by solvent; (iii) the decrease in rates of chemical reactions within the film environment, e.g., the slowness of the aquation of Ru^{II}–chloro and Ru^{II}–ONO_2 sites, of nitro/nitrosyl interconversion and of H/D exchange at Ru^{II}–aquo sites.

Acknowledgments are made to the Army Research Office—Durham under Grant No. DAAG29-79-C-0044 for support of this research and to Dr. Royce W. Murray, Dr. Derek Hodgson, and John Facci for helpful discussions.

Registry No. $[Ru(bpy)_2(vpy)(N_3)](PF_6)$, 82731-41-7; $[Ru(bpy)_2(py)(CN)](PF_6)$, 82740-43-0; *cis*-$Ru(bpy)_2(PVP)_2^{2+}$, 82769-08-2; $Ru(bpy)_2(PVP)(OH_2)^{2+}$, 75931-35-0; $Ru(bpy)_2(PVP)(CN)^{+}$, 82731-42-8; $Ru(bpy)_2(PVP)Cl^{+}$, 75675-25-1; $Ru(bpy)_2(PVP)(CH_3CN)^{2+}$, 80864-62-6; $Ru(bpy)_2(PVP)(NO_2)^{+}$, 80864-61-5; $Ru(bpy)_2(PVP)(NO)^{3+}$, 82731-43-9; $Ru(bpy)_2(PVP)(NO_3)^{+}$, 82731-44-0; $Ru(bpy)_2(PVP)(N_3)^{+}$, 82731-40-6; $Ru(bpy)_2(PVP)(OH)^{+}$, 82731-45-1; $Ru(bpy)_2(py)_2^{2+}$, 63338-38-5; $Ru(bpy)_2(py)(CN)^{+}$, 82731-46-2; $Ru(bpy)_2(py)Cl^{+}$, 33519-09-4; $Ru(bpy)_2(py)(CH_3CN)^{2+}$, 82769-09-3; $Ru(bpy)_2(py)(NO_2)^{+}$, 34398-55-5; $Ru(bpy)_2(py)(NO)^{3+}$, 82769-10-6; $Ru(bpy)_2(py)(NO_3)^{+}$, 82769-11-7; $Ru(bpy)_2(py)(N_3)^{+}$, 82769-12-8; $Ru(bpy)_2(py)(OH_2)^{2+}$, 67202-42-0; $Ru(bpy)_2(py)(OH)^{+}$, 75495-06-6; *cis*-$Ru(bpy)_2Cl_2$, 19542-80-4; $[Ru(bpy)_2(py)Cl]PF_6$, 62387-78-4; $[Ru(bpy)_2(py)(OH_2)](PF_6)_2$, 75495-09-9; $Ru(bpy)_2(CO_3)$, 59460-48-9.

Contribution from the Department of Chemistry, Brookhaven National Laboratory, Upton, New York 11973

Nature of Bis(2,2′-bipyridine)rhodium(I) in Aqueous Solutions

MEI CHOU, CAROL CREUTZ,* DEVINDER MAHAJAN, NORMAN SUTIN, and ARDEN P. ZIPP

Received December 29, 1981

Spectrophotometric studies of aqueous solutions of bis(2,2′-bipyridine)rhodium(I) ($Rh(bpy)_2^{+}$) as a function of pH and rhodium(I) concentration provide evidence for four species as shown in eq 1–3. At room temperature log K_1 = 4.0 ± 0.2, log K_2 = 7.3 ± 0.1, and log K_3 = 9.3 ± 0.3. Both monomer and dimer in eq 1 are purple; λ_{max}(monomer) = 505 nm ($\epsilon \approx 1.0 \times 10^4$ M^{-1} cm^{-1}) and λ_{max}(dimer) ≈ 530 nm (ϵ/rhodium ≈ 1.0×10^4 M^{-1} cm^{-1}). The rhodium(III) hydride (eq 2) does not absorb in the visible region but the "protonated dimer" (eq 3) is brown: λ_{max} (ϵ/rhodium) = 960 nm (2.3×10^3 M^{-1} cm^{-1}), ~500 nm (4.2×10^3 M^{-1} cm^{-1}, sh), 420 nm (4.8×10^3 M^{-1} cm^{-1}). The properties elucidated for these species are compared with those of other d^8 systems.

$$2Rh(bpy)_2^{+} \rightleftharpoons [Rh(bpy)_2]_2^{2+} \quad (1)$$

$$Rh(bpy)_2^{+} + H_3O^{+} \rightleftharpoons Rh(bpy)_2(H)H_2O^{2+} \quad (2)$$

$$[Rh(bpy)_2]_2^{2+} + H^{+} \rightleftharpoons [Rh(bpy)_2]_2H^{3+} \quad (3)$$

The preparation of purple salts and solutions containing bis(2,2′-bipyridine)rhodium(I) species was first reported by Waind and Martin in 1958;[1,2] the results of more extensive magnetic measurements and the spectral properties of dilute ethanolic solutions were reported subsequently.[3] Interest in the reactivity and the nature of these species in aqueous solution has recently been stimulated by the results of photochemical experiments in which water is reduced to hydrogen.[4-7] Bis(2,2′-bipyridine)rhodium(I) ($Rh(bpy)_2^{+}$) was found to be a product in some of the experiments and has been postulated to be a reactive intermediate in hydrogen formation under some conditions.[8-10] Preliminary results[6] indicated the nature

(1) Waind, G. M.; Martin, B. *J. Inorg. Nucl. Chem.* **1958**, *8*, 551.
(2) Martin, B.; Waind, G. M. *Proc. R. Soc. London* **1958**, 169.
(3) Martin, B.; McWhinnie, W. R.; Waind, G. M. *J. Inorg. Nucl. Chem.* **1961**, *23*, 207.
(4) Lehn, J.-M.; Sauvage, J.-P. *Nouv. J. Chim.* **1977**, *1*, 449.
(5) Kirch, M.; Lehn, J.-M.; Sauvage, J.-P. *Helv. Chim. Acta* **1979**, *62*, 1345.
(6) Brown, G. M.; Chan, S.-F.; Creutz, C.; Schwarz, H. A.; Sutin, N. *J. Am. Chem. Soc.* **1979**, *101*, 7639.
(7) Chan, S.-F.; Chou, M.; Creutz, C.; Matsubara, T.; Sutin, N. *J. Am. Chem. Soc.* **1981**, *103*, 369.
(8) The original postulate that $Rh(bpy)_2^{+}$ reduces water to hydrogen over platinum[4,5] at pH 7–8 has been shown to be incorrect. There is, however, evidence[5,7,9,10] that $Rh(bpy)_2(H)(H_2O)^{2+}$ may provide a catalyst for reduction of water by $Rh(bpy)_3^{2+}$ in more acidic solutions.

0020-1669/82/1321-3989$01.25/0

of "$Rh(bpy)_2^{+}$" in aqueous solution to be a function of both pH and rhodium(I) concentration. Here we report the results of spectrophotometric experiments over a range of conditions and present evidence for at least four rhodium species.

Experimental Section

Materials. AR grade solvents were used without further purification but were vacuum-degassed before use. Rhodium trichloride hydrate was purchased from Alfa.

Rhodium Compounds. All of the Rh(I) solids and solutions were manipulated under argon with use of glovebox or Schlenk techniques.[11] The preparation of millimolar stock $Rh(bpy)_2^{+}$ solutions by the electrolytic reduction of $Rh(bpy)_2(OH)_2^{+}$ (sulfate salt) in aqueous alkali has been described.[2] This remains the method of choice for the preparation of relatively concentrated aqueous solutions. Several routes to the salts $[Rh(bpy)_2]Cl$ and $[Rh(bpy)_2]ClO_4$ are known[3,12] but the products are not too soluble in water. For work in organic solvents $[Rh(bpy)_2]Cl$ is useful, and the following procedure yields this material in high yield.

$[RhL_2]Cl$ (L = bpy, phen). The cyclooctene dimer $[RhCl(C_8H_{14})]_2$ was prepared by a literature method.[13] A benzene solution (10 mL) of 2.2 mmol of the ligand (0.344 g of bpy or 0.436 g of phen) was added to a red solution of $[RhCl(C_8H_{14})_2]_2$ (0.5 mmol, 0.358 g) under argon. A deep purple complex formed immediately and was collected on a filter, washed three times with benzene, and dried in vacuo (yield ~90%). The complexes were stored under argon. Anal. Calcd[14] for $RhC_{20}H_{16}N_4Cl$ (L = bpy): C, 53.27; H, 3.55; N, 12.43; Cl, 7.88; Rh, 22.83. Found: C, 50.33; H, 3.56; N, 11.12; Cl, 7.30; Rh, 23.10. Calcd[14] for $RhC_{24}H_{16}N_4Cl$ (L = phen): C, 57.72; H, 3.21; N, 11.22; Cl, 7.10; Rh, 20.62. Found: C, 56.61; H, 3.63; N, 11.20; Cl, 6.50; Rh, 19.2.

$[Rh(bpy)(H)Cl_2]_2$. To a purple suspension of $[RhL_2]Cl$ (L = bpy or phen) in ethanol (0.5 mmol in 100 mL) was added 5 mL of 12 M HCl. The solution became green immediately. After 0.5 h of stirring, the solution was yellow and a green solid separated. The solid was filtered, washed with ethanol a few times, and dried in vacuo. Anal. Calcd[14] for $Rh_2C_{20}H_{18}N_2Cl_2$ (L = bpy): C, 36.25; H, 2.72; N, 8.46; Cl, 21.45; Rh, 31.12. Found: C, 36.59; H, 3.07; N, 11.04; Cl, 20.2; Rh, 26.8. IR: ν(Rh–H) 2140 cm^{-1}; ν(Rh–Cl or Rh–N) 325, 305 cm^{-1}.

$[RhL_2(H)Cl]Cl$ (L = bpy, phen). The yellow filtrate from above was evaporated to dryness, and the yellow residue was dissolved in CH_2Cl_2 (3 mL). Diethyl ether was added slowly to yield yellow crystals of the desired hydride product. The complexes were stored under argon. Anal. Calcd[14] for $RhC_{20}H_{17}N_4Cl_2$ (L = bpy): C, 49.25; H, 3.49; N, 11.49; Cl, 14.57; Rh, 21.12. Found: C, 44.84; H, 3.88; N, 10.61; Cl, 18.3; Rh, 21.4. IR: ν(Rh–H) 2070 cm^{-1} (Nujol mull). Anal. Calcd[14] for $RhC_{24}H_{17}N_4Cl_2$ (L = phen): C, 53.83; H, 3.18; N, 10.47; Cl, 13.27; Rh, 19.23. Found: C, 47.46; H, 3.15; N, 9.05; Cl, 17.4; Rh, 16.5. IR: ν(Rh–H) 2090 cm^{-1} (Nujol mull). The high Cl analyses are due to the presence of CH_2Cl_2. The CH_2Cl_2 resonance was detected in proton NMR spectra and, with L = bpy, indicated the solid to contain ~6% CH_2Cl_2.

$[Rh(bpy)_2(D)Cl]Cl$. To a purple suspension of $[Rh(bpy)_2]Cl$ (70 mg) in C_2H_5OD (10 mL) was added 1 mL of DCl (38% w/w in D_2O). On ~0.5 h of stirring, a green solid precipitated. The solid was filtered, and the yellow filtrate was evaporated to dryness. The crude solid was crystallized from dry CH_2Cl_2–ether.

Methods. Recourse to a number of inert-atmosphere techniques was necessary in performing the spectral studies of Rh(I) solutions. The work with aqueous solutions more concentrated than $\sim 0.5 \times 10^{-4}$ M in Rh(I) was carried out with syringe techniques; known volumes of $\sim 2 \times 10^{-3}$ M Rh(I) stock solutions were added to premeasured, deaerated buffer contained in spectrophotometer cells topped by large-bore glass stopcocks capped with a septum. After the addition of the Rh(I) through the septum and stopcock, the needle was withdrawn and the stopcock was closed. In experiments where it was desirable to measure UV and visible spectra of the same solution, a stopcock–U-tube attached to two (e.g., 2 mm and 1 cm) cells was employed. After the visible scan was complete, the solution was tipped to fill the shorter path length cell for the UV scan. Glovebox techniques were essential for the study of solutions $(0.01–1) \times 10^{-5}$ M in Rh(I). The glovebox used was a stainless steel, three-glove Vacuum Atmospheres Model HE-493 modified to permit connection of leads from pH, SCE, and graphite electrodes to a Metrohm 632 pH meter and a Princeton Applied Research Model 176 potentiostat–galvanostat and a Model 175 universal programmer outside the box. So that work with aqueous solutions could be faciliated, the bulk of the molecular sieve usually used in the Dri-Train was replaced with Ridox. Stock Rh(I) solutions were prepared by electrolysis within the box[7] and diluted with use of automatic pipets into volumetric flasks. The pH of the resulting solution was measured, and the solution was transferred to a 1–10-cm cell and sealed with a greased ground-glass stopper. For the spectral measurements with nonaqueous solvents, $[Rh(bpy)_2]Cl$ was weighed on a Sartorius 1207 MP2 balance located in the glovebox, diluted to known volume, and transferred to cells equipped with ground-glass stoppers. Argon was used as blanket gas in all the experiments.

Spectra were recorded on a Nicolet MX-1 FT IR or a Beckman Acculab 10 (for IR, solid samples were run as Nujol mulls between CsI plates), a Varian CFT-20 (for NMR), and a Cary 17 or a Cary 210 (for UV–vis) spectrophotometer. Microanalyses were performed by Schwarzkopf Microanalytical Laboratory and by Ms. E. Norton of this department.

Results

Alkaline aqueous solutions of bis(2,2′-bipyridine)rhodium(I), regardless of origin and concentration, are purple. The color arises from an intense absorption band centered at 500–530 nm ($\epsilon = \epsilon/Rh(I) \approx 10^4$ M^{-1} cm^{-1}). At very high concentrations a near-IR band ($\lambda_{max} = 1100$ nm, $\epsilon \approx 1 \times 10^3$ M^{-1} cm^{-1}) is seen. Intense ($\epsilon \approx 2.5 \times 10^4$ M^{-1} cm^{-1}) UV absorption bands are observed at ~245 and ~300 nm, and a shoulder is observed at 360 nm. In 0.05 M sodium hydroxide these UV–visible spectral features persist throughout the Rh(I) concentration range investigated, 0.5×10^{-6} to 2.0×10^{-3} M. The detailed behavior of the visible band is, however, disconcerting: The latter shifts gradually from $\lambda_{max} \approx 505$ nm at [Rh(I)] = $(0.03–\sim 0.3) \times 10^{-5}$ M to $\lambda_{max} \approx 528$ nm at [Rh(I)] $\approx 10^{-3}$ M. (These, as well as comparable data for 0.10 M NaOH, are given in Supplementary Tables I and II.) This shift is shown at the top of Figure 1, where λ_{max} is plotted against the concentration of Rh(I). Over the entire concentration range the effective molar absorptivity in this wavelength region remains nearly constant. This is illustrated at the bottom of Figure 1, where the absorbance per 1-cm path length at 505 and 530 nm is plotted against the rhodium(I) concentration. Beer's law is very nearly followed at both wavelengths. It is to be noted, however, that at high concentration the 505-nm points (filled circles) fall *below* the line (solid line) extrapolated from the low-concentration points and that the 530-nm points (open circles) extrapolated from high to low concentration (broken line) yield a nonzero intercept (see insert). Reactions involving dissociation of bpy at low [Rh(I)] do not appear to be involved: the spectra of $(1–5) \times 10^{-6}$ M Rh(I) in 0.01 M sodium hydroxide are the same in the presence and absence of 1.1×10^{-4} M bpy. Furthermore, bpy addition (to give $Rh(bpy)_3^{+}$) is not observed. At 1×10^{-4} M Rh(I) no spectral changes are observed upon the addition of bpy to the 1×10^{-3} M level in 0.05 M sodium hydroxide.

Pronounced spectral changes are observed, however, as the acidity of the medium is increased. As is shown in Figure 2, at very low Rh(I) concentration the absorption at $\lambda > 350$ nm decreases as the pH decreases, with the bleaching being essentially complete at pH 6. By contrast, at higher Rh(I) concentration (see Figure 3), the bleaching of the visible (515–525-nm) absorption band which occurs between pH 10 and 8 is accompanied by the growth of new absorption features

(9) Mulazanni, D. G.; Emmi, S.; Hoffman, M. Z.; Venturi, M. *J. Am. Chem. Soc.* **1981**, *103*, 3362.
(10) Hoffman, M. Z. *ACS Symp. Ser.*, in press.
(11) Shriver, D. F. "Manipulation of Air Sensitive Compounds"; McGraw-Hill: New York, 1969.
(12) Oliver, F. D.; Miller, J. D. *J. Chem. Soc., Dalton Trans.* **1972**, 2473.
(13) van der Ent, A.; Onderlinden, A. L. *Inorg. Synth.* **1973**, *14*, 92.
(14) The solvent of crystallization has not been included in the calculated values.

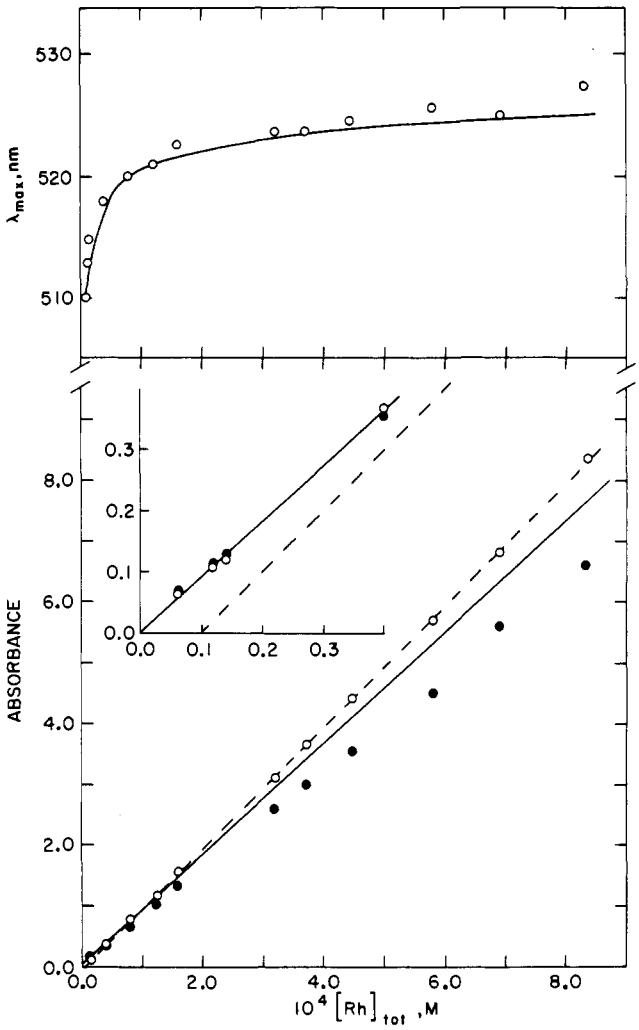

Figure 1. Spectral features of "$Rh(bpy)_2^{+n}$" solutions in 0.05 M NaOH as a function of concentration: (top) absorption maximum of the visible band; (bottom) absorbance per centimeter at 505 (solid circles) and 530 nm (open circles).

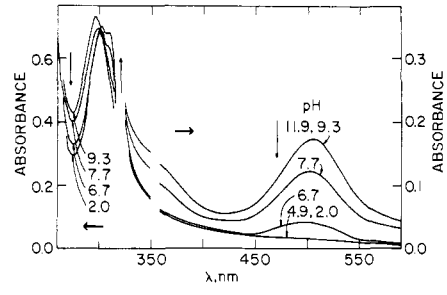

Figure 2. Spectra of 0.2×10^{-5} M $Rh(bpy)_2^+$ solutions in 10-cm cells at pH 11.9 (NaOH), 9.3 (triethanolamine–sulfate buffer), 7.7 (triethanolamine–sulfate, sodium phosphate buffer), 6.7 (sodium phosphate buffer), 4.9 (acetate buffer), and 2.0 (sulfuric acid) at 0.01 M ionic strength and room temperature.

at 420 and ~930 nm. The dependence of the intensities of these bands on Rh(I) concentration at pH 8–10 is shown in Figure 4. The acid–base behavior of the solution appears completely reversible. Brown neutral concentrated solutions (as in Figure 3) and colorless neutral dilute solutions (as in Figure 2) of Rh(I) are both rapidly restored to their purple color upon the addition of oxygen-free concentrated sodium hydroxide. The latter changes are complete in a few minutes or less. However, addition of concentrated alkaline Rh(I) solutions to solutions buffered at pH <7 gives rise to a slower change, with bleaching in the visible region occurring over 5–30

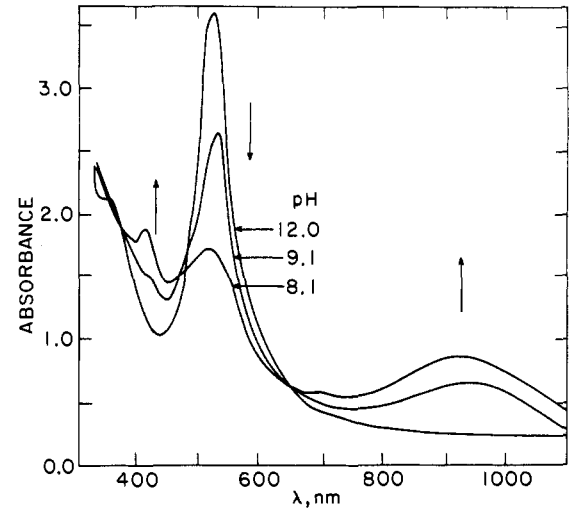

Figure 3. Spectra (absorbance per centimeter vs. λ in nm) of 0.4×10^{-3} M "$Rh(bpy)_2^{+n}$" solutions at pH 12 (NaOH), 9.1 (borate buffer), and 8.1 (Tris buffer) at room temperature.

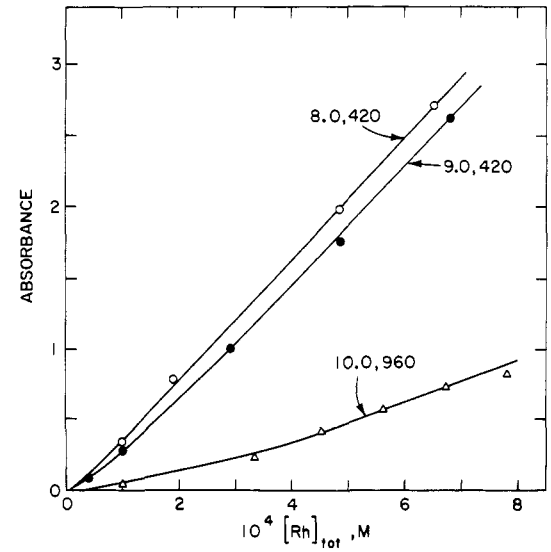

Figure 4. Absorbance per centimeter of "$Rh(bpy)_2^{+n}$" as a function of concentration at 420 nm and pH 8.0 (open circles), 420 nm and pH 9.0 (filled circles), and 960 nm and pH 10.0 (triangles).

Table I. The 420-nm Absorbance per Centimeter of Acidic "$Rh(bpy)_2^{+n}$" Solutions at Room Temperature[a]

10^4[Rh]$_{tot}$, M	pH	buffer	A_{420}
2.32	5.00	acetate	0.61
3.51	4.98	acetate	1.04
4.69	5.02	acetate	1.56
7.15	5.05	acetate	2.40
0.87	5.80	phosphate	0.24
1.74	6.05	phosphate	0.61
6.10	5.88	phosphate	2.50
0.83	6.90	phosphate	0.34
1.84	7.17	Tris	0.81
3.68	6.92	phosphate	1.62

[a] Sulfuric acid was added to neutralize NaOH in the Rh(I) stock solution. The buffer concentration ranged from 0.03 to 0.1 M and the ionic strength from 0.08 to 0.13 M.

min, depending upon [Rh(I)] and pH. The behavior of the 420-nm band in the pH range 5–7 is summarized in Table I. The absorbance values reported there are for solutions in which these slow changes are complete.

Molar Absorptivities of Rh(I) Solutions. The molar absorptivity of the 500–530-nm band for $Rh(bpy)_2^+$ solutions

Table II. UV-Visible Spectra of $[RhL_2]Cl$ and $[RhL_2(H)Cl]Cl$

compd	10^4[Rh], M	medium	λ_{max}, nm ($10^{-4}\epsilon$, M^{-1} cm^{-1})
$[Rh(bpy)_2]Cl$	10.0	ethanol	555 (1.26), 520 (sh, 0.99)
	10.0	7:3 (v/v) ethanol-H_2O	552 (1.21), 526 (1.14)
	10.0	3:7 (v/v) ethanol-H_2O	524 (1.10)
	5.3	ethanol	555 (1.26), 520 (sh, 0.74), 365 (0.68), 298 (3.28), 243 (2.75)
	4.8	methanol	555 (1.25), 520 (sh, 0.83), 365 (0.73), 298 (4.17), 243 (3.77)
	4.0	dimethylacetamide	555, 515 (sh), 365, 300, 284[a]
	4.0	dichloromethane	reaction with solvent–yellow solution
	3.3	0.1 M aq NaOH	523 (0.91)
$[Rh(bpy)_2(H)Cl]Cl$[b]	2.4	0.1 M aq HCl	308 (4.3), 248 (4.8)
	2.0	methanol	310 (3.2), 303 (sh, 2.9), 247 (3.5)
	5.5	0.1 M aq NaOH	523 (0.76), 360 (sh, 0.47), 294 (1.78), 243 (1.84)
$[Rh(phen)_2Cl]$	2.6	ethanol	562 (1.14), 525 (sh), 455 (sh), 290 (sh), 272 (3.44), 260 (sh)
	4.0	0.1 M aq NaOH	535 (0.85), 267 (3.00)
$[Rh(phen)_2(H)Cl]Cl$[b]	2.6	0.1 M aq HCl	273 (5.5)
	4.1	0.5 M aq H_2SO_4	273 (4.6)
	2.2	methanol	273 (4.8)
	3.7	0.1 M aq NaOH	535 (0.6), 273 (3.2)

[a] Before slow reaction with solvent. [b] These materials contain residual CH_2Cl_2, and the ~15% low ϵ values in 0.1 M NaOH are attributed to the fact that no correction has been made for this factor.

is $\sim 10^4$ M^{-1} cm^{-1}. On the basis of the number of coulombs passed during electrolysis of $Rh(bpy)_2(OH)_2^+$ we first reported $\epsilon_{518} = 8600 \pm 800$ M^{-1} cm^{-1} for $\sim 1 \times 10^{-4}$ M $Rh(bpy)_2^+$ in 0.05 M NaOH.[6] Subsequently we found $\epsilon_{521} = (1.1 \pm 0.1) \times 10^4$ M^{-1} cm^{-1} in 0.05 M NaOH from the reaction of 2×10^{-4} M Rh(I) with methylviologen (MV^{2+}; the molar absorptivity of the methylviologen radical produced was taken as $(1.1 \pm 0.1) \times 10^4$ M^{-1} cm^{-1} at 605 nm).[7] Mulazanni et al. recently reported $\epsilon_{518} = 9.5 \times 10^3$ M^{-1} cm^{-1} at pH 11 from reduction of $Rh(bpy)_3Cl_3$ with $NaBH_4$.[9] In the present study we obtained $\epsilon_{523} = (1.03 \pm 0.05) \times 10^4$ M^{-1} cm^{-1} in 0.05 M NaOH from $S_2O_8^{2-}$ oxidation of 3×10^{-4} M $Rh(bpy)_2^+$ (assuming the reaction consumes 1 $Rh(I)/S_2O_8^{2-}$) and $\epsilon_{523} = 9.1 \times 10^3$ M^{-1} cm^{-1} for 3.3×10^{-4} M $[Rh(bpy)_2]Cl$ dissolved in 0.10 M NaOH. Thus at $\lambda \approx 520$ nm, $\epsilon_{max} = (1.1 \pm 0.1) \times 10^4$ M^{-1} cm^{-1} is consistent with all the observations on alkaline $(1-3) \times 10^{-4}$ M $Rh(bpy)_2^+$ solutions.

As will be seen later, the value of the visible molar absorptivity in the low Rh(I) concentrations is an important parameter in any quantitative model of the spectral behavior. In particular, the magnitude of ϵ_{505} in the $\sim(0.3-2.4) \times 10^{-6}$ M Rh(I) range over which λ_{max} is [Rh(I)] independent is crucial. Exact evaluation proved extremely difficult (using even the most careful glovebox techniques), not only because of minute residual levels of O_2 but also because of trace impurities in the reagents used. Thus identical dilutions of stock Rh(I) diluted to $\sim 1.5 \times 10^{-6}$ M with Milli-Q water, 0.01 M NaOH, and 0.10 M NaOH gave A_{505} values (per 10-cm path length) of 0.132, 0.128, and 0.062, respectively, implicating the presence of $\sim 1 \times 10^{-6}$ M oxidant in the 0.1 M NaOH. It was for this reason that all the experiments with $<10^{-5}$ M Rh(I) were performed with dilute (~0.01 M) buffers and sodium hydroxide. Unfortunately, this limited the ionic strength range that could be encompassed. In an attempt to eliminate complications from residual oxidants, the methylviologen and $S_2O_8^{2-}$ approaches to the determination of ϵ (as described above) were employed. With methylviologen $\epsilon_{505} = (8.7 \pm 0.8) \times 10^3$ M^{-1} cm^{-1} was found, but here a slow increase in the MV^+ absorption proved a complicating feature. With $S_2O_8^{2-}$ as oxidant the somewhat larger value $\epsilon_{505} = (9.1 \pm 1.0) \times 10^3$ M^{-1} cm^{-1} was obtained. Although the magnitude of ϵ for the visible maximum at low Rh(I) is somewhat smaller than that for 100-fold higher concentrations (at longer wavelength), the difference is probably not significant in view of the difficulties intrinsic to the low-concentration measurements.

UV–visible spectra obtained for $[RhL_2]Cl$ and $[RhL_2(H)Cl]Cl$ are given in Table II. No emission was observed from aqueous or ethanolic $[Rh(bpy)_2]Cl$ solutions. The visible spectrum of $[Rh(bpy)_2]Cl$ (2×10^{-4} M) in ethanol–water mixtures is a function of the composition of the mixture. As shown in Table II, as the water content increases from zero to 30% to 70%, the 520-nm "shoulder" first increases relative to the 555-nm peak and in the 70% water solution only a single peak with $\lambda_{max} = 520$ nm is found.

No hydride signals were seen in the NMR spectra of $[RhL_2(H)Cl]Cl$ in the τ 10–50 range; the aromatic protons appeared as complex multiplets (L = bpy: Me_2SO-d_6, $\delta \sim$ 9.8–7.3; CD_3OD, δ 9.9–7.36. L = phen: CD_3OD, δ 9.95–7.5).

The green solid $[Rh(bpy)(H)Cl_2]_2$ obtained as a byproduct in the preparation of $[Rh(bpy)_2(H)Cl]Cl$ was found to dissolve only in aqueous alkali, with which it reacted to give a gray solution. Over a period of days it reacted with added bpy (0.1–1 mM) to give the spectrum of $Rh(bpy)_2^+$ (Table II).

In passing, we mention some other observations bearing on the reactivity of "$Rh(bpy)_2^+$" in its various forms. The purple alkaline forms are rapidly oxidized by O_2, $Os(bpy)_3^{3+}$, and methylviologen (*N*,*N*′-dimethyl-4,4′-bipyridine) cation. These reactions are complete within ~15 s of mixing the reactants at the 10^{-4} M level. By contrast, reaction of the colorless acid form with $Os(bpy)_3^{3+}$ under comparable conditions requires >10 h in 0.01 M H_2SO_4. Ligand replacement is facile in base: the spectrum of $Rh(bpy)_2^+$ mixed at the 10^{-5} M level with 10^{-4} M L = 4,7-diphenylphenanthroline sulfonate was converted to that of RhL_2^+ in less than 20 min. By contrast, in 0.01 M H_2SO_4 no loss of bpy was detected in 10^{-5} M solutions after 10 days.

We also find that $[Rh(bpy)_2]Cl$ provides an efficient water-gas shift catalyst in 2-methoxyethanol at 90 °C.[15]

In preliminary experiments, the reaction of $[Rh(bpy)_2]Cl$ with H_2 was investigated. With ethanol as solvent, exposure of a $[Rh(bpy)_2]Cl$ solution to H_2 (1 atm) led to rapid, nearly quantitative (>80%) bleaching of the purple color in the absence and presence of $<10^{-2}$ M bpy. Removal of the H_2 gas (evacuation) resulted in restoration of the 555-nm band intensity in several minutes. Similar observations were made for aqueous solutions of 3×10^{-4} M Rh(I) at pH >12, but the extent of reaction appeared smaller (~25% bleaching). At pH 7 (phosphate buffer), however, addition of H_2 to the brown Rh(I) solution produced a deep blue solution. The blue color persisted after removal of the H_2 gas, but adjustment of the solution to pH >12 produced the purple shade characteristic of $Rh(bpy)_2^+$ under these conditions.

(15) Mahajan, D., to be submitted for publication.

Discussion

So that the spectral behavior seen in Figures 1–4 and in the organic solvents (Table II) can be accounted for, at least four "$Rh(bpy)_2^{+n}$" species are required. We first present an overall scheme (Scheme I) describing the aqueous system and then turn to the detailed analysis of the observations in terms of this scheme. The form present at very low Rh(I) in alkaline solution is postulated to be the monomer $Rh(bpy)_2^+$ or $Rh(bpy)_2(H_2O)^+$ (vide infra).[16] As the total Rh(I) concentration is increased, association takes place to give the dimer $[Rh(bpy)_2]_2^{2+}$ (eq 1). Lowering the pH at low Rh(I) results in protonation of the monomer (oxidative addition of H_3O^+) with $Rh(bpy)_2(H)(H_2O)^{2+}$, the colorless rhodium(III) hydride, as the product (eq 2). By contrast, lowering the pH at very high Rh(I) gives the brown protonated dimer $[Rh(bpy)_2]_2H^{3+}$ (eq 3).

Scheme I

$$2Rh(bpy)_2^+ \overset{K_1}{\rightleftharpoons} [Rh(bpy)_2]_2^{2+} \quad (1)$$

$$Rh(bpy)_2^+ + H_3O^+ \overset{K_2}{\rightleftharpoons} Rh(bpy)_2(H)(H_2O)^{2+} \quad (2)$$

$$[Rh(bpy)_2]_2^{2+} + H^+ \overset{K_3}{\rightleftharpoons} [Rh(bpy)_2]_2H^{3+} \quad (3)$$

At very low [Rh(I)] and intermediate (high, i.e., pH 8) pH, eq 4 (from a combination of eq 1 and 3) is relevant, while at

$$2Rh(bpy)_2^+ + H^+ \overset{K_4}{\rightleftharpoons} [Rh(bpy)_2]_2H^{3+} \quad (4)$$

high [Rh(I)] and intermediate (low, i.e., pH 6) pH, eq 5 (obtained by combining eq 1–3) describes the predominant species present.

$$2Rh(bpy)_2(H)(H_2O)^{2+} \overset{K_5}{\rightleftharpoons} [Rh(bpy)_2]_2H^{3+} + H_3O^+ + H_2O \quad (5)$$

Monomer–Dimer Equilibrium. The shift in the visible λ_{max} to longer wavelengths can be explained by eq 1 if the monomer and dimer are assumed to have very similar (but slightly displaced) spectra. Since the spectrum is concentration independent, with λ_{max} = 505 nm below $\sim 3 \times 10^{-6}$ M Rh(I), this is taken as the monomer spectrum. As is evident in Figure 1, after changing rapidly between 10^{-5} and 10^{-4} M Rh(I), λ_{max} still shifts somewhat between 10^{-4} and 10^{-3} M but appears to level off near 530 nm. Over the entire range of concentrations ϵ_{max} is $\sim 10^4$ M^{-1} cm^{-1}. Consequently, we postulate that the monomer and dimer have λ_{max} of 505 and $\sim$530 nm, respectively, with the values of the molar absorptivity (per Rh(I)) being nearly the same ($\sim 10^4$ M^{-1} cm^{-1}) at the respective maxima. That such a small displacement of the λ_{max} values does give rise to gradual shifts in the observed maximum as the composition of the solution changes *without any pronounced change in band shape* is illustrated in Figure 5. In constructing Figure 5 experimental spectra obtained at 3×10^{-6} M Rh(I) (monomer) and 1.8×10^{-3} M (dimer) were normalized to $\epsilon_{max} = 1.0 \times 10^4$ M^{-1} cm^{-1} (solid curves) and added and normalized to give the spectrum of a mixture 50% in monomer and 50% in dimer (on the basis of total [Rh(I)]). The calculated spectrum (dashed curve) is very similar in shape and width to the monomer and dimer spectra. The λ_{max} observed (519 nm) is similar to that found experimentally for $\sim 10^{-4}$ M solutions at high pH. This model gives rise to reasonable spectral shifts for other monomer–dimer compositions, and in fact, the solid curve shown at the top of Figure 1 was calculated from the above assumptions and K_1 = 1.3 $\times 10^4$ M^{-1}. It is apparent that the above interpretation provides a good description of the observed behavior.

(16) Except in the case of $Rh(bpy)_2(H)H_2O^{2+}$, which is assumed to be six-coordinate Rh(III), coordinated water molecules are generally omitted from the formulas for the sake of brevity and because their presence is not definitely established by our results.

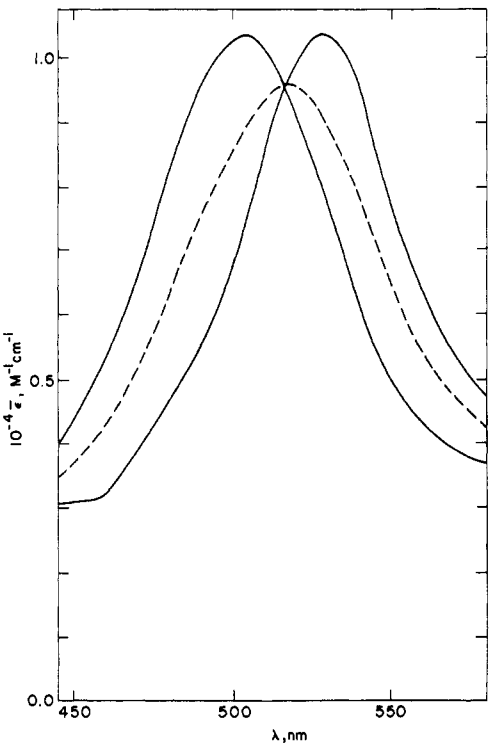

Figure 5. Simulated spectrum (dashed curve) of $Rh(bpy)_2^+$–$[Rh(bpy)_2]_2^{2+}$ 1:0.5 mixture based on monomer and dimer maxima of 505 and 530 nm, respectively (solid curves).

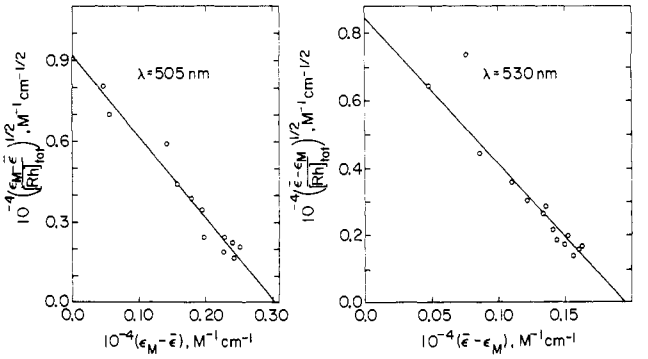

Figure 6. Left: plot of $[(\epsilon_M - \bar{\epsilon})/[Rh]_{tot}]^{1/2}$ vs. $(\epsilon_M - \bar{\epsilon})$ for "$Rh(bpy)_2^{+n}$" in 0.05 M NaOH at 505 nm ($\epsilon_M = 1.03 \times 10^4$ M^{-1} cm^{-1}). Right: plot of $[(\bar{\epsilon} - \epsilon_M)/[Rh]_{tot}]^{1/2}$ vs. $(\bar{\epsilon} - \epsilon_M)$ at 530 nm ($\epsilon_M = 0.83 \times 10^4$ M^{-1} cm^{-1}).

In order to treat quantitatively the magnitudes of the absorbance changes shown at the bottom of Figure 1 and estimate K_1, we use a treatment outlined by Schwarz et al.[17] Here the absorbance measured at a given wavelength A_{tot} is the sum of monomer and dimer absorbances (eq 6) with C_M and C_D

$$A_{tot} = \bar{\epsilon}[Rh]_{tot} = \epsilon_M C_M + 2\epsilon_D C_D \quad (6)$$

$$[Rh]_{tot} = C_M + 2C_D$$

being the equilibrium concentrations of $Rh(bpy)_2^+$ and $[Rh(bpy)_2]_2^{2+}$, respectively, and ϵ_M and ϵ_D being the respective molar absorptivities *per Rh(I)*. At equilibrium eq 7 applies.

$$C_D = K_1 C_M^2 \quad (7)$$

We introduce $\Delta\epsilon = (\epsilon_M - \epsilon_D)$ where $\epsilon_M > \epsilon_D$ and use eq 8 to

$$[(\epsilon_M - \bar{\epsilon})/[Rh]_{tot}]^{1/2} = (2K_1/\Delta\epsilon)^{1/2}[\Delta\epsilon - (\epsilon_M - \bar{\epsilon})] \quad (8)$$

(17) Schwarz, G.; Klose, S.; Balthasar, W. *Eur. J. Biochem.* **1970**, *12*, 454.

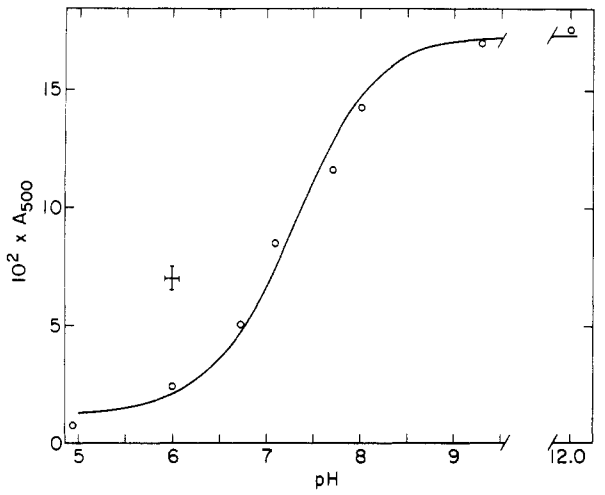

Figure 7. Absorbance per centimeter at 500 nm of 0.2×10^{-5} M "$Rh(bpy)_2^{+}$" as a function of pH at $\mu = 0.01$ M and room temperature. The curve is drawn for $K_2 = 2 \times 10^7$ M^{-1}. See Figure 2 for buffers used.

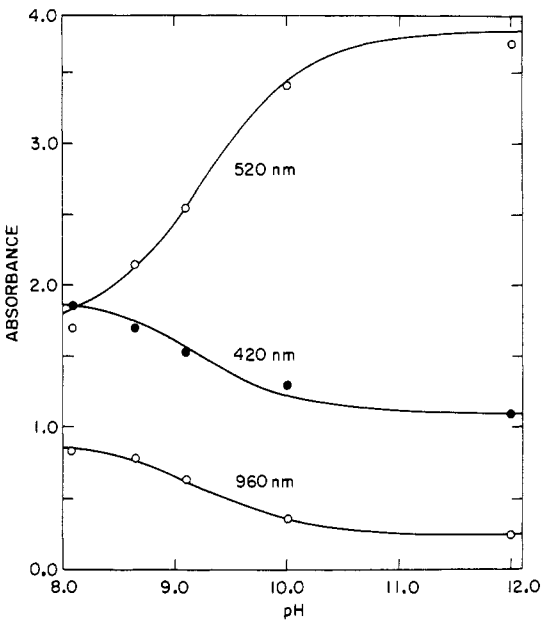

Figure 8. Plots of absorbance per centimeter as a function of pH for 0.4×10^{-3} M "$Rh(bpy)_2^{+}$" at 520 nm (open circles), 420 nm (filled circles), and 960 nm (bottom, open circles). The curves are drawn for $K_3 = 1.78 \times 10^9$ M^{-1} and ϵ values summarized in Table III.

treat the data obtained at 505 nm. A plot of $[(\epsilon_M - \bar{\epsilon})/[Rh]_{tot}]^{1/2}$ vs. $(\epsilon_M - \bar{\epsilon})$ should thus be linear with y and x intercepts of $(2K_1(\Delta\epsilon))^{1/2}$ and $\Delta\epsilon$, respectively. Such a plot for the 0.05 M NaOH 505-nm data is shown at the left-hand side of Figure 6. The value used for ϵ_M was 1.03×10^4 M^{-1} cm^{-1}; the parameters then obtained are $\epsilon_D = 0.73 \times 10^4$ M^{-1} cm^{-1} and $K_1 = 1.39 \times 10^4$ M^{-1}. Since $\epsilon_D > \epsilon_M$ at 530 nm, we define $\Delta\epsilon = \epsilon_D - \epsilon_M$ and employ eq 9. The plot resulting for

$$[(\bar{\epsilon} - \epsilon_M)/[Rh]_{tot}]^{1/2} = (2K_1/\Delta\epsilon)^{1/2}[\Delta\epsilon - (\bar{\epsilon} - \epsilon_M)] \quad (9)$$

the 530-nm data with $\epsilon_M = 0.83 \times 10^4$ M^{-1} cm^{-1} is shown at the left-hand side of Figure 6 and yields $\epsilon_D = 1.03 \times 10^4$ M^{-1} cm^{-1} and $K_1 = 1.72 \times 10^4$ M^{-1}. Comparable analysis of the data for 0.10 M NaOH (Supplementary Table II) with $\epsilon_M = 1.03 \times 10^4$ M^{-1} cm^{-1} at 500 nm yields $\epsilon_D = 0.52 \times 10^4$ M^{-1} cm^{-1} and $K_1 = 0.68 \times 10^4$ M^{-1} while $\epsilon_M = 0.75 \times 10^4$ M^{-1} cm^{-1} at 540 nm yields $\epsilon_D = 0.89 \times 10^4$ M^{-1} cm^{-1} and $K_1 = 0.69 \times 10^4$ M^{-1}. The uncertainties associated with K_1 evaluated in this manner are considerable. Very small (<10%) changes in trial ϵ_M values can lead to K_1 values that differ by a factor of 2. Thus the agreement between the 505- and 530-nm K_1 values for 0.05 M NaOH must be regarded as satisfactory and the lower values of the K_1 values for 0.05 M NaOH are not necessarily significant.

Monomer–Hydride Equilibrium. Acidification of very dilute Rh(I) solutions is accompanied by bleaching of the visible absorption bands. Equation 2, protonation of Rh(I) or oxidative addition of H_3O^+ to monomeric Rh(I), is proposed to account for this observation. The absorbance at 500 nm for a 0.2×10^{-5} M Rh(I) solution as a function of pH is shown in Figure 7; the curve is drawn for $K_2 = 2.0 \times 10^7$ M^{-1}. Consistent with the formulation of the colorless species as a rhodium(III) hydride are the properties of $[Rh(bpy)_2(H)Cl]Cl$ isolated from the addition of concentrated HCl to ethanolic $[Rh(bpy)_2]Cl$. This solid is yellow and manifests a metal–hydride stretching frequency at 2070 cm^{-1}. This band is absent for $[Rh(bpy)_2(D)Cl]Cl$, and the M–D stretch is apparently obscured by bpy absorption in the 1400–1500-cm^{-1} region. While dissolution of these solids in alcohol or acidic aqueous solution yields a colorless to light yellow solution with strong absorption only in the UV region (Table II), dissolution in 0.1 M NaOH results in a purple solution with λ_{max} and ϵ_{max} nearly identical with that of $Rh(bpy)_2^{+}$ (or $[Rh(bpy)_2]Cl$, see Table II) at the same rhodium concentration. We have not, however, detected a hydride resonance in the NMR spectra of $[Rh(bpy)_2(H)Cl]Cl$. This failure is presumably due to facile exchange of M–H with the solvent, in the case of methanol-d_4 solvent, to give M–D. For Me_2SO as solvent, the lack of hydride resonance remains unexplained.

Dimer–Protonated Dimer Equilibrium. In Figure 3 the spectral changes occurring when the pH of 4×10^{-4} M Rh(I) is lowered were introduced. In Figure 8 the absorbance changes at 520, 420, and 960 nm are plotted against pH. The curves are drawn for eq 3 with $K_3 = 1.78 \times 10^9$ M^{-1} ($pK_a = 9.25$). This data treatment is not completely justified since the formation of dimer is not complete at 4×10^{-4} M $[Rh]_{tot}$. With the assumption of $K_3 = 1.78 \times 10^9$ M^{-1} and $K_1 = 1 \times 10^4$ M^{-1} the fraction of Rh(I) remaining as monomer (eq 1) at 4×10^{-4} M is 28% at pH 10, 25% at pH 9, and 7.8% at pH 8. Because of this complication from eq 1, K_3 obtained by this method is likely to be underestimated ($K_3 > 1.8 \times 10^9$, $pK_a > 9.25$). Since solubility problems precluded systematic investigation of eq 3 at higher Rh(I) concentrations where eq 1 would lie further to the right, this equilibrium was examined indirectly through the related equation (5) and data obtained at pH 5–7 (Table I) were used as a further test of Scheme I. The ϵ values 0.475×10^4 and 0.09×10^4 M^{-1} cm^{-1} at 420 nm were used for $[Rh(bpy)_2]_2H^{3+}$ and $Rh(bpy)_2(H)H_2O^{2+}$, and the quotient Q, defined by $Q = [[Rh(bpy)_2]_2H^{3+}]/[Rh(bpy)_2(H)(H_2O)^{2+}]^2$, suggested by eq 5 was calculated by assuming only eq 5 to be relevant. The results obtained are shown in Figure 9, where log Q is plotted vs. pH. The line drawn through the points is given by $\log Q = 0.89pH - 0.95$. The broken line in Figure 9 is that calculated, i.e.

$$\log Q = 1.0pH + \log (K_1K_3/K_2^2) \quad (10)$$

If a line of slope 1.0 is imposed on the points, the intercept log K_5 obtained is ~ -1.5 whereas the value calculated from eq 10 is −1.35 (K_5(obsd) = 3.2×10^{-2}; K_5(calcd) = 4.5×10^{-2}). Such agreement is quite acceptable in view of the fact that K_2 was determined at much lower ionic strength. In addition there is a substantial uncertainty in both K_1 and K_3. The fact that the "observed" K_5 is smaller than that calculated could, however, be due to a low estimate for K_3 as discussed above.

The results of the data treatments leading to evaluation of equilibrium constants for eq 1–5 are summarized in Table III. All the equilibria are expected to be a function of ionic strength. Unfortunately it proved experimentally impossible

Table III. Summary of Parameters Obtained for Scheme I[a]

	log K	10^4[Rh]$_{tot}$, M	medium	λ, nm	$10^{-4}\epsilon_R$, M^{-1} cm^{-1}	$10^{-4}\epsilon_P$, M^{-1} cm^{-1}
$2Rh(bpy)_2^+ \rightleftharpoons [Rh(bpy)_2]_2^{2+}$	4.14	0.1–20	0.05 M NaOH	505	1.03	0.73
	4.24			530	0.83	1.03
	3.83	0.5–17.5	0.10 M NaOH	500	1.03	0.52
	3.84			540	0.75	0.89
$Rh(bpy)_2^+ + H_3O^+ \rightleftharpoons Rh(bpy)_2(H)H_2O^{2+}$	7.30	0.02	μ = 0.01 M, pH 2–12	500	1.03	0.075
$[Rh(bpy)_2]_2^{2+} + H^+ \rightleftharpoons [Rh(bpy)_2]_2H^{3+}$	9.25	4.0	μ = 0.05–0.1 M, pH 8–12	420	0.275	0.475
				520	0.950	0.425
				960	0.0625	0.225
$2Rh(bpy)_2(H)H_2O^{2+} \rightleftharpoons [Rh(bpy)_2]_2H^{3+} + H_3O^+$	(−1.5)[b]	0.8–7.2	μ = 0.05–0.1 M, pH 5–7	420	0.09	0.475

[a] The entries ϵ_R and ϵ_P are the molar absorptivities (per rhodium) of the reactant and product. [b] The relationship between log Q, where $Q = [[Rh(bpy)_2]_2H^{3+}]/[Rh(bpy)_2(H)H_2O^{2+}]^2$, and pH is found to be log Q = 0.89pH − 0.95 whereas that calculated from the first three entries in this table is log Q = 1.0pH − 1.35. The value −1.5 tabulated was obtained by imposing a slope of 1.0 as described in the text.

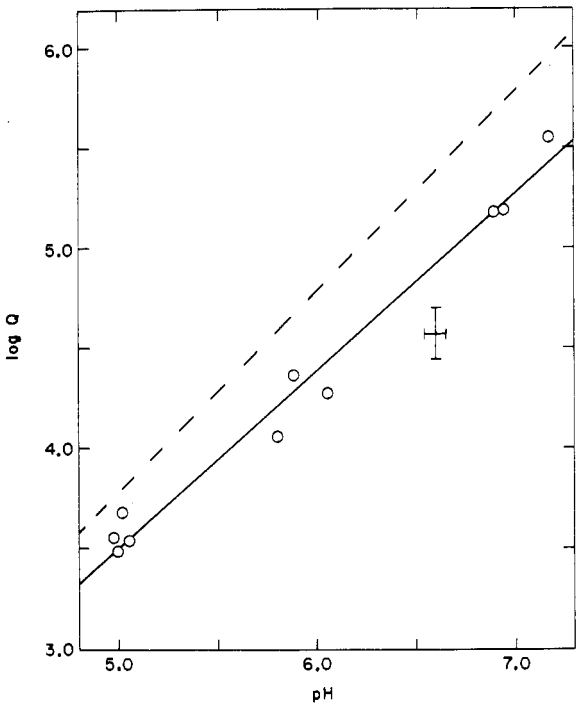

Figure 9. Plot of log Q, where $Q = [[Rh(bpy)_2]_2H^{3+}]/[Rh(bpy)_2(H)(H_2O)^{2+}]^2$, vs. pH (open circles) for the data in Table I. The solid line is given by log Q = 0.89pH − 0.95. The broken line is that calculated from log Q = 1.0pH + log (K_1K_3/K_2^2).

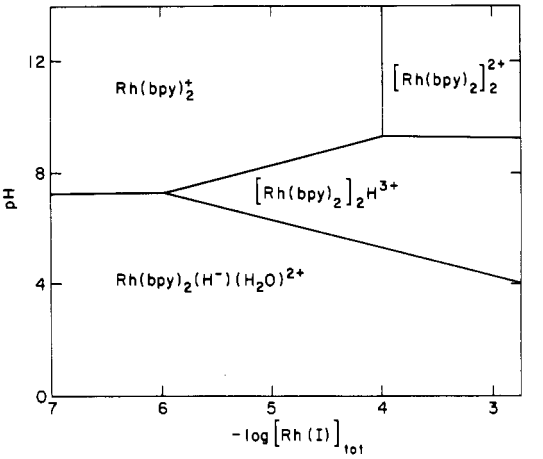

Figure 10. Dominant species in aqueous "$Rh(bpy)_2^+$" solutions as a function of the logarithm of $[Rh(I)]_{tot}$ and pH. The lines between the zones are drawn at the 50:50 points, i.e., when $2[[Rh(bpy)_2]_2^{2+}] = [Rh(bpy)_2^+]$, etc.

to investigate all the limiting cases at the same ionic strength. Furthermore, in view of the other experimental problems (oxygen sensitivity and solubility), it is unlikely that the uncertainties in any of the K values are less than ~30%. Thus the agreement between the "composite" value K_5 and its constituents K_1, K_2, and K_3 is reasonably good, and eq 1–5 represent a semiquantitatively useful description of the system over a substantial range of conditions. It is, however, to be noted that Scheme I and Table III do not provide a complete description of the system under all conditions: *Not* treated in this model are the transient green species obtained upon acidification of concentrated, alkaline Rh(I) stock solutions. In addition, at pH 7–5 the maximum of the near-IR band shifts gradually to shorter wavelength with increasing acidity. Finally, alkaline >2 × 10^{-3} M Rh(I) solutions manifest visible maxima beyond 530 nm (presumably due to further oligomerization of Rh(I), e.g., trimer or tetramer formation). Explanation of the last observations is outside the scope of the present work. With these limitations of the model in mind, we summarize our observations in Figure 10, which shows the dominant species present in aqueous solution as a function of the total Rh(I) concentration and pH. The lines between the zones are drawn at 50:50 points; i.e., the vertical line separating the $Rh(bpy)_2^+$ and $[Rh(bpy)_2]_2^{2+}$ zones is drawn for the condition $2[[Rh(bpy)_2]_2^{2+}] = [Rh(bpy)_2^+]$. Above pH 9.25, these are the predominant forms. At lower pH, $[Rh(bpy)_2]_2H^{3+}$ persists over a wide range of pH and $[Rh]_{tot}$, giving way to $Rh(bpy)_2(H)H_2O^{2+}$ at a pH depending on the value of $[Rh]_{tot}$.

Comparisons with Other Systems. The species present in water at low $[Rh(I)]_{tot}$ and high pH is four-coordinate $Rh(bpy)_2^+$ with square-planar[18] or tetrahedrally distorted square-planar geometry[19] or five-coordinate $Rh(bpy)_2(H_2O)^+$. The absorption spectrum of this monomer manifests maxima at 295 and 505 nm, with a shoulder at ~350 nm. The 295-nm band is ascribed to a bpy-centered π–π^* transition and the 350- and 500-nm bands to Rh(I) d to bpy π^* metal-to-ligand charge-transfer (MLCT) transitions. This spectrum differs in several aspects from that reported for $[Rh(bpy)_2]ClO_4$ in aqueous ethanol[1-3] (λ_{max} 285 nm for 10^{-5} M solutions and λ_{max} 557 nm, shoulder 520 nm, for >10^{-4} M solutions) and from that seen here for $[Rh(bpy)_2]Cl$ in ethanol and methanol (see Table II). The alcoholic solutions of both salts exhibit shoulders at ~520 nm and maxima at ~555 nm and do not change in the [Rh(I)] range (5–500) × 10^{-6} M. The behavior in mixed solvents (Table II) suggests (a) dissociation of

(18) Durham, B.; Wilson, R. S.; Hodgson, D. J.; Meyer, T. J. *J. Am. Chem. Soc.* **1980**, *102*, 600.
(19) Chieh, P. C. *J. Chem. Soc., Dalton Trans.* **1972**, 1643. Vu Dong; Endres, H.; Keller, H. J.; Moroni, W.; Nothe, D. *Acta Crystallogr., Sect. B* **1977**, *B33*, 2428. Endres, H.; Keller, H. J.; Moroni, W.; Nothe, D.; Vu Dong. *Ibid.* **1978**, *B34*, 1823. Nakai, H. *Bull. Chem. Soc. Jpn.* **1971**, *44*, 2412.

five-coordinate $Rh(bpy)_2Cl$ (dominant form in alcohol) to $Rh(bpy)_2^+$ and Cl^- as water is added, or (b) reaction of $Rh(bpy)_2^+$ (dominant form in alcohol) with water to give five-coordinate $Rh(bpy)_2H_2O^+$, or (c) aquation of $Rh(bpy)_2Cl$ to give $Rh(bpy)_2H_2O^+$. Alternative b is supported by the observation that $[Rh(bpy)_2]ClO_4$ is a 1:1 electrolyte in ethanol[3] and by the counterion independence of the spectrum in ethanol. If indeed $Rh(bpy)_2H_2O^+$ is the dominant form in water, Scheme I should be modified to take this into account with eq 1 and 2 written with the five-coordinate species as reactant and water molecules as products to balance the equation. Such a formulation does not in any other way affect the modeling of the pH- and [Rh(I)]-dependent equilibria.[20]

Oligomerization of d^8 complexes is a well-established phenomenon,[21-25] and association constants for dimerization reactions analogous to eq 1 have now been reported for several systems in aqueous media. The value obtained here $K_1 = (1.0 \pm 0.6) \times 10^4\ M^{-1}$ for 0.05–0.1 M ionic strength with monomer (M) = $Rh(bpy)_2^+$ is somewhat greater than with M = $Rh(CNR)_4^+$ (R = *tert*-butyl, $K = 0.25 \times 10^3\ M^{-1}$, $\mu = 0.1$ M)[23] and comparable to the dimerization constants for M = $Rh_2(TMB)_4Rh_4^{8+}$ (TMB = 2,5-dimethyl-2,5-diisocyanohexane, $Rh_4^{6+} = [Rh_2(1,3\text{-diisocyanopropane})_4]_4^{6+}$, $K = 1.8 \times 10^4\ M^{-1}$ in 1 N H_2SO_4)[21] and for $Pt(terpy)X^+$ (terpy = 2,2′,2″-terpyridine; for X = Cl^-, $K = (4 \pm 2) \times 10^3\ M^{-1}$ at $\mu = 0.1$ M, and for x = 2-hydroxyethanethiolate, $K = (7 \pm 2) \times 10^3\ M^{-1}$).[25] The impetus for these association reactions is formation of a (weak) metal–metal bond[22] and, for the platinum terpyridine complexes, hydrophobic ("stacking") interactions between the ligands[25] as well. It is conceivable that both kinds of interaction contribute to the stability of $[Rh(bpy)_2]_2^{2+}$ since eclipsing of the bpy's on the monomer units could provide a favorable stacking interaction with overlap of metal-centered d orbitals contributing to a weak Rh(I)–Rh(I) bond. It is noteworthy that the superficial features of the spectral shifts observed for $Rh(bpy)_2^+$ dimerization may suggest a greater contribution from the former than the latter. For $Pt(terpy)X^+$ "stacking", the relative intensities (but not the positions) of the various electronic absorption bands were found to change. Similarly, only small spectral changes (Figure 1) accompany the dimerization of $Rh(bpy)_2^+$. By contrast, in the various $Rh(CNR)_4^+$ (R = alkyl group) oligomerization systems studied, very pronounced spectral shifts occur; e.g., the position of the longest wavelength maximum seen for R = *tert*-butyl with H_2O as solvent is for $[Rh(CNR)_4]_n^{n+}$ 371 nm (n = 1), 490 nm (n = 2), and 622 nm (n = 3).[23] These striking changes have been accounted for in terms of the shifts that occur in the energies of the lowest unoccupied and highest occupied molecular orbitals when association occurs. The LUMO in both monomer and oligomer is predominantly d_{z^2} in character, while the HOMO is an admixture of metal p_z and ligand π^*. Oligomerization lowers the LUMO and raises the HOMO so that the transition between them shifts to lower energy with increasing oligomerization. Thus the fact that only small shifts are found for $Rh(bpy)_2^+$ could be ascribed to a much weaker Rh(I)–Rh(I) interaction than in the isocyanide series. It should, however, be noted that the MO description for the monomer building blocks may differ qualitatively, as well as quantitatively, between the bpy and –CNR series since the bpy LUMO is substantially lower in energy than the LUMO for –CNR. As a consequence, it is expected that the bpy π^* orbital may be significantly mixed with d_{xz} and d_{yz} in the ground state and that the LUMO is largely bpy π^* (little contribution from Rh p_z) in the excited state. As a result, the lowest transition for $Rh(bpy)_2^+$ is more metal-to-ligand charge transfer (MLCT) than metal centered in character and the effects of dimerization on such a transition may be small.

While rhodium(III) hydrides such as $Rh(bpy)_2(H)(H_2O)^{2+}$, $Rh(NH_3)_5(H)^{2+}$, $Rh(PR_3)(H)Cl^+$, etc. abound, few data comparable to those obtained here for eq 2 ($pK_a(Rh(bpy)_2(H)(H_2O)^{2+}) = 7.3$) are available. The pK_a recorded for the dimethylglyoxime complex $Rh(dmgH)_2P(C_6H_5)_3(H)$ in 1:1 methanol–water is 9.5.[26] Among the other hydrides characterized in aqueous solution, the saturated amine complexes $Rh(NH_3)_4(H)(H_2O)^{2+}$ and $Rh(en)_2(H)(H_2O)^{2+}$ appear much less acidic, with pK_a values of 14 or greater,[27,28] while the isocyanide complexes $Rh(CNR)_4(H)(H_2O)^{2+}$ appear much more acidic ($pK_a < 0$).[21,23] Similarly, rhodium(III) dihydrides, implicated here in the reaction of $Rh(bpy)_2^+$ with H_2 in ethanolic and aqueous solutions, are known to form rapidly and reversibly in a number of systems.[29,30] Our preliminary experiments suggest that no bpy is lost from the coordination sphere when reaction with H_2 occurs but do not clarify the nature of the dominant form of the rhodium product in the solutions; i.e., eq 11, H_2 addition, could be followed by deprotonation, eq 12. In aqueous base and in ethanol, reaction

$$Rh(bpy)_2^+ + H_2 \rightleftharpoons Rh(bpy)_2H_2^+ \quad (11)$$

$$Rh(bpy)_2H_2^+ + OH^- \rightleftharpoons Rh(bpy)_2H^0 + H_2O \quad (12)$$

with H_2 leads to a nearly colorless solution and so suggests $Rh(bpy)_2H_2^+$, a rhodium(III) dihydride, as product. The nature of the blue pH 7 species is unknown. These observations have implications for a number of other systems since the intermediacy of (bipyridine)rhodium(III) dihydrides has been invoked in the reduction of $Rh(bpy)_2Cl_2^+$ by ethanol,[12] the hydrogenation of olefins,[31] and the homogeneous photoreduction of water.[5,7-10]

In contrast to the rhodium(III) mono- and dihydrides discussed above, there appear to be no precedents in rhodium chemistry for the species we postulate to be $[Rh(bpy)_2]_2H^{3+}$, a "protonated rhodium(I) dimer". Species possessing the structural unit

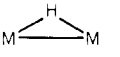

(20) A reviewer has suggested that the hydroxy complex $Rh(bpy)_2OH$ may be relevant. We reject deprotonation of $Rh(bpy)_2H_2O^+$, i.e.

$$Rh(bpy)_2H_2O^+ \rightleftharpoons Rh(bpy)_2OH + H^+$$

as responsible for the $pK = 7.3$ equilibrium described as eq 2 for several reasons. First, it is not reasonable that $Rh(bpy)_2H_2O^+$ would be colorless in water when $Rh(bpy)_2X$ dissolved in ethanol, etc. is purple. Furthermore, water bound to Rh(I) is not likely to be this acidic. The pK_a's of the six-coordinate Rh(III) and Rh(II) species $Rh(bpy)_2(H_2O)_2^{3+}$ and $Rh(bpy)_2(H_2O)_2^{2+}$ are 4.8 and 6.87 and 8.6 and 11.1 (Schwarz, H. A., unpublished results), respectively. It is, however, possible that $Rh(bpy)_2H_2O^+$ (if present) deprotonates above pH 13 ($Rh(bpy)_2OH$ is present when $[OH^-] > 0.1$ M), a region we have not investigated. It is also worth mentioning that deprotonation of water bound to $Rh(bpy)_2(H)(H_2O)^{2+}$ (pK likely 7–9) should give $Rh(bpy)_2(H)(OH)^+$, which is "isomeric" (and possibly in equilibrium) with $Rh(bpy)_2(H_2O)^+$. At present we have no information bearing on the latter equilibrium.

(21) Sigal, I. S.; Gray, H. B. *J. Am. Chem. Soc.* **1981**, *103*, 2220.
(22) Mann, K. R.; Gordon, J. G., II; Gray, H. B. *J. Am. Chem. Soc.* **1975**, *97*, 3553.
(23) Mann, K. R.; Lewis, N. S.; Williams, R. M.; Gray, H. B.; Gordon, J. G., II. *Inorg. Chem.* **1978**, *17*, 828.
(24) Geoffroy, G. L.; Bradley, M. G.; Keeney, M. E. *Inorg. Chem.* **1978**, *17*, 777.
(25) Jennette, K. W.; Gill, J. T.; Sadownick, J. A.; Lippard, S. J. *J. Am. Chem. Soc.* **1976**, *98*, 6159.
(26) Ramasani, T.; Espenson, J. H. *Inorg. Chem.* **1980**, *19*, 1846.
(27) Thomas, K.; Osborn, J. A.; Powell, A. R.; Wilkinson, G. *J. Chem. Soc. A* **1968**, 1801.
(28) Thomas, K.; Wilkinson, G. *J. Chem. Soc. A* **1970**, 356.
(29) Schrock, R. R.; Osborn, J. A. *J. Am. Chem. Soc.* **1971**, *93*, 2397.
(30) James, B. R.; Mahajan, D. *Can. J. Chem.* **1980**, *58*, 996.
(31) Zassinovich, G.; Camus, A.; Mestroni, G. *Inorg. Nucl. Chem. Lett.* **1976**, *12*, 865.

are, however, known for other metal centers.[32] It should be noted that eq 3 is written as it is because the new spectral features (bands at 420 and 960 nm) grow at low $[Rh(I)]_{tot}$ as $[Rh(I)]_{tot}^2$ and $[H^+]$. Because of the ambiguities associated with water as solvent, the overall reaction eq 1 + eq 3 could equally well be written as eq 13 or eq 14, in which OH^- is a

$$2Rh(bpy)_2(OH)_2^- + H^+ \rightleftharpoons [Rh(bpy)_2(OH)]_2OH^- + H_2O \quad (13)$$

$$2Rh(bpy)_2OH + H^+ \rightleftharpoons [Rh(bpy)_2]_2OH^+ + H_2O \quad (14)$$

bridging ligand. These would, however, require six- and five-coordinate hydroxy complexes as the dominant form of mononuclear Rh(I), a possibility we reject[20] since the spectrum of Rh(I) at very low concentrations is $[OH^-]$ independent above pH 7 (an exceptionally large affinity of $Rh(bpy)_2^+$ for OH^- or acidity for $Rh(bpy)_2(H_2O)^+$ or $Rh(bpy)_2(H_2O)_2^+$ would be required). Furthermore, the IR spectra of brown solids isolated from neutral solutions of $[Rh(bpy)_2]Cl$ show no absorption in the O–H stretching region. No M–H stretch is observed for these solids either, but none would be expected in the 2000-cm^{-1} region for the bridged structure postulated. Presumably the true nature of this dimer may be resolved through X-ray crystallographic methods, and efforts to grow crystals of this species are ongoing.

(32) See: Bau, R.; Teller, R. G.; Kirtley, S. W.; Koetzle, T. F. *Acc. Chem. Res.* **1979**, *12*, 176 and references cited therein.

Conclusions

The nature of aqueous $Rh(bpy)_2^+$ solutions is a function of the hydrogen ion and rhodium(I) concentrations, with four species formulated as $Rh(bpy)_2^+$, $[Rh(bpy)_2]_2^{2+}$, $[Rh(bpy)_2]_2H^{3+}$, and $Rh(bpy)_2(H)(H_2O)^{2+}$ being required to account for the spectral changes that accompany acidification and/or dilution of the solutions. Equilibration between the species is achieved rapidly, but strongly acid solutions of $Rh(bpy)_2(H)(H_2O)^{2+}$ are much less reactive toward ligand exchange and oxidation, as expected for rhodium(III), than are the basic solutions containing rhodium(I).

Acknowledgment. Helpful comments from Drs. G. M. Brown, H. B. Gray, and J. Halpern are gratefully acknowledged. We thank Dr. M. Andrews for his comments and for running the NMR spectra. This research was carried out at Brookhaven National Laboratory under contract with the U.S. Department of Energy and supported by its Office of Basic Energy Sciences.

Registry No. $[Rh(bpy)_2]Cl$, 17633-22-6; $[Rh(phen)_2]Cl$, 82752-94-1; $[Rh(bpy)(H)Cl_2]_2$, 82752-95-2; $[Rh(bpy)_2(H)Cl]Cl$, 82752-96-3; $[Rh(phen)_2(H)Cl]Cl$, 82752-97-4; $[Rh(bpy)_2(D)Cl]Cl$, 82752-98-5; $[RhCl(C_8H_{14})_2]$, 12279-09-3.

Supplementary Material Available: Tables of absorbance data for various concentrations of $Rh(bpy)_2^+$ in 0.05 and 0.1 M NaOH (2 pages). Ordering information is given on any current masthead page.

Contribution from the Department of Chemistry, Stanford University, Stanford, California 94305

Isocyanide as a Ligand on Ruthenium(II) Ammines

L. DOZSA, J. E. SUTTON, and H. TAUBE*

Received January 12, 1982

A pentaammine–isocyanide complex of Ru(II) is readily prepared by the reaction of $Ru(NH_3)_5H_2O^{2+}$ with the ligand, but if the contact time is long, a *trans*-bis(isocyanide) complex results. Measurement of the rate of aquation of the benzyl isocyanide complex $Ru(NH_3)_5C_7H_7NC^{2+}$ compared with earlier measurements for $Ru(NH_3)_6^{2+}$ shows that C_7H_7NC (as compared to ammonia) labilizes a trans ammonia by a factor of 40. A similar comparison between $Ru(NH_3)_4(H_2O)C_7H_7NC^{2+}$, now following the replacement of H_2O by isn (isonicotinamide), shows that the trans isocyanide (compared to trans ammonia) is slightly delabilizing. The rate of aquation of isn in a trans position is enormously enhanced by isocyanide as compared to ammonia, and the affinity of Ru(II) for isn is much reduced. As determined by cyclic voltammetry, the values of E_f for the couples $Ru(NH_3)_5C_7H_7NC^{3+/2+}$, $Ru(NH_3)_4(H_2O)C_7H_7NC^{3+/2+}$, *trans*-$Ru(NH_3)_4(C_7H_7NC)_2^{3+/2+}$, and *trans*-$Ru(NH_3)_4(c\text{-}HxNC)_2^{3+/2+}$ are 0.79, 0.92, 0.99, and 0.93 V vs. NHE at 25 °C.

The specific rates for substitution in pentaammineaquoruthenium(II) by neutral ligands at 25 °C lie in the range[1] 0.02–0.3 M^{-1} s^{-1}. The species $Ru(NH_3)_5H_2O^{2+}$ however is a rather strong reducing agent (E_f = 0.051 V);[2] for some applications, namely, in certain catalytic processes, it is desirable to have a couple that has a much higher value of E_f, but with the Ru(II) form substitutionally labile so that a high turnover number is realized in reaction with dioxygen or another oxidant.[3] While E_f for the Ru(III)/Ru(II) couple is readily increased by replacing saturated ligands with π acids, for many of the π acids commonly used this is at the expense of substitution lability.[4] Thus, while substitution of H_2O on $Ru(NH_3)_5H_2O^{2+}$ by isn (isonicotinamide) takes place at a specific rate of 1.0×10^{-1} M^{-1} s^{-1} at 25 °C, when the trans or cis ammonias are replaced by isn, the specific rates fall to 3.5×10^{-3} or 5.0×10^{-3} m^{-1} s^{-1}, respectively.[4] There are some ligands however, among them SO_3^{2-}, which in replacing NH_3 on Ru(II) cause an increase in E_f yet labilize the trans ligand.[5] These ligands seem to constitute a distinct class,[6] but just what features of electronic structure distinguish them from saturated or π-acid ligands such as pyridine are not understood. The existence of ligands such as SO_3^{2-} however does offer some hope that a high substitution lability in Ru(II) is not incompatible with a high value of E_f for the Ru(III)/Ru(II) couple. Preliminary preparative work with an isocyanide acting on $Ru(NH_3)_5H_2O^{2+}$ showed that the reaction readily yields a *trans*-bis(isocyanide) complex, thus suggesting trans labilization by a ligand ordinarily considered a strong π acid.[7] This finding is described in this paper, as are the results of the more complete study prompted by it.

A large number of isocyanide complexes of ruthenium(II) have been reported,[8,9] but in most cases more than one π-acid

(1) Taube, H. *Comments Inorg. Chem.* **1981**, *1*, 17.
(2) Matsubara, T.; Ford, P. C. *Inorg. Chem.* **1976**, *15*, 1107.
(3) A metal complex to be useful as a catalyst for the O_2 electrode should have a value of $E_f \sim 1.0$ V and a turnover number of 10^2–10^3 s^{-1} for oxygen in a saturated solution in equilibrium with the atmosphere.
(4) Isied, S. S.; Taube, H. *Inorg. Chem.* **1976**, *15*, 3070.
(5) Isied, S. S.; Taube, H. *Inorg. Chem.* **1974**, *13*, 1545.
(6) Tweedle, M. F.; Taube, H., in preparation (quoted in ref 1).
(7) Sutton, J. E. Ph.D. Thesis, Stanford University, 1980.

0020-1669/82/1321-3997$01.25/0